Response of R&S faults to stress perturbations

***

Supplementary material

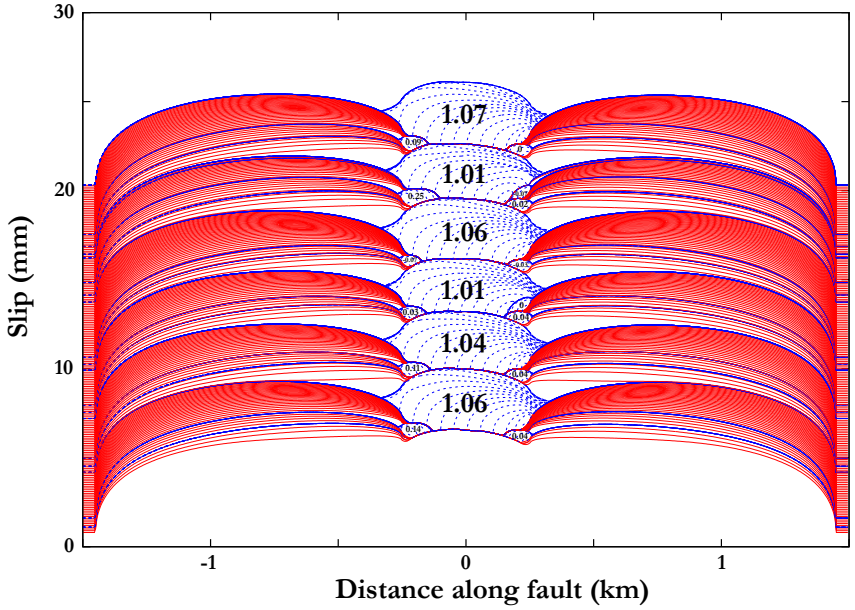

Figure S1: Slip on the fault presented in section 4, when the fault undergoes a harmonic perturbation at period $T = 0.0027$ years. The red lines are plotted every 0.01 year during the interseismic period, while the blue dashed lines are plotted every 0.02 s when seismic rupture is occurring, i.e. when the maximum velocity on the fault is greater than 1cm/s. This pattern of slip is to be compared to the slip on the unperturbed fault presented in Figure 4a. Once the fault is perturbed, the seismicity only consists of large $M_{\text{lin}} \approx 1.05$ events followed by two small ($-0.4 \leq M_{\text{lin}} \leq 0.4$) aftershocks, and sometimes a small foreshock. The ratio of small to large events in this case is 2.25, indicating that, on average, there is a foreshock every 4 cycles. This well-organized pattern of seismicity is very different from the seismicity on the unperturbed fault.

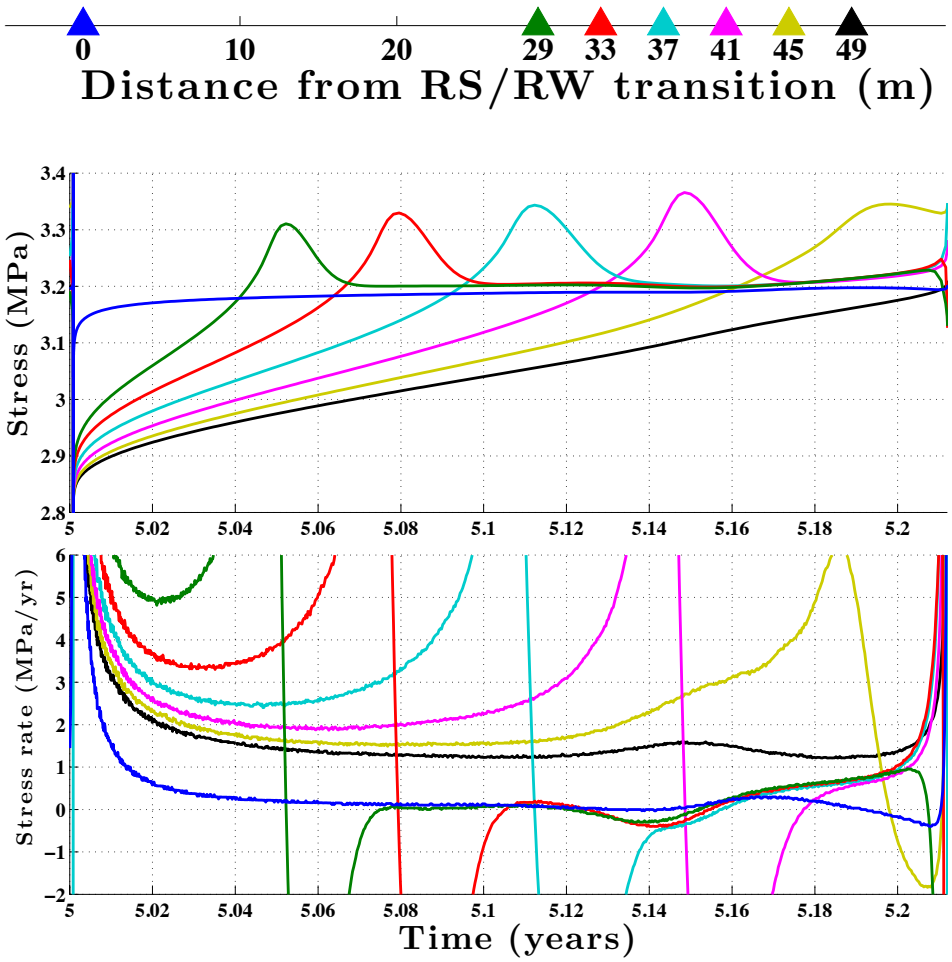

Figure S2: Evolution of the stress and stress rate with time in the nucleation zone, for the unperturbed fault model with the response of Figure 4a. The shear stress and its time derivative are plotted at 7 points, one at the rate-weakening/rate-strengthening transition (blue curve), and 6 others located inside the rate-weakening zone between 29 m and 49 m from the rate-strengthening/rate-weakening transition, equally spaced by 4 m from one another. The position of the points at which the stress is measured is indicated on the upper plot. At each of the points, the stress increases as the nucleation-zone tip progresses toward the measurement point, and then decreases to a common value once the point is within a creeping nucleation zone. The time at which the stress is maximum can be defined as the instant at which the nucleation-zone tip is at the measurement point. The lower plot shows that the stress rate in the nucleation zone varies with time and localization within the nucleation zone, but that it is always larger than 1.25 MPa/yr (black line). The rupture nucleates when the crack tip is located between 45 and 49 m within the nucleation zone, which gives the critical nucleation size.

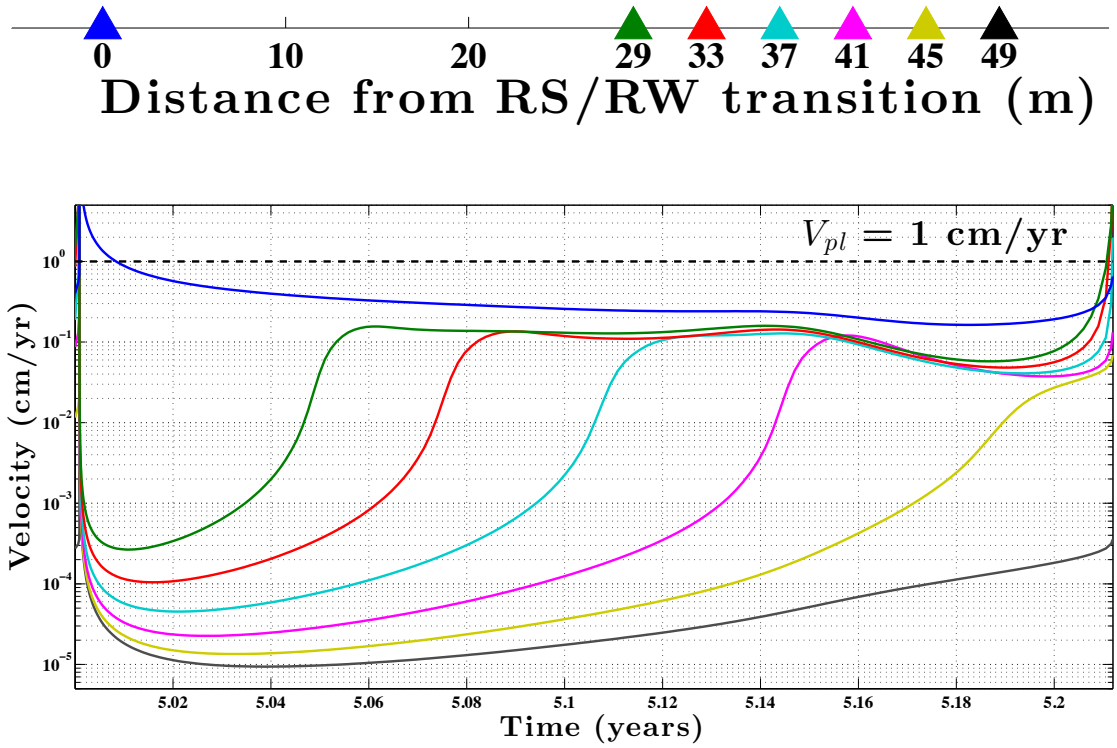

Figure S3: Evolution of the slip velocity with time in the nucleation zone, at the same locations as in Figure S2. The slip velocity in the nucleation zone is lower than the remote plate loading rate of $V_{pl} = 1$ cm/yr for most of the nucleation time.

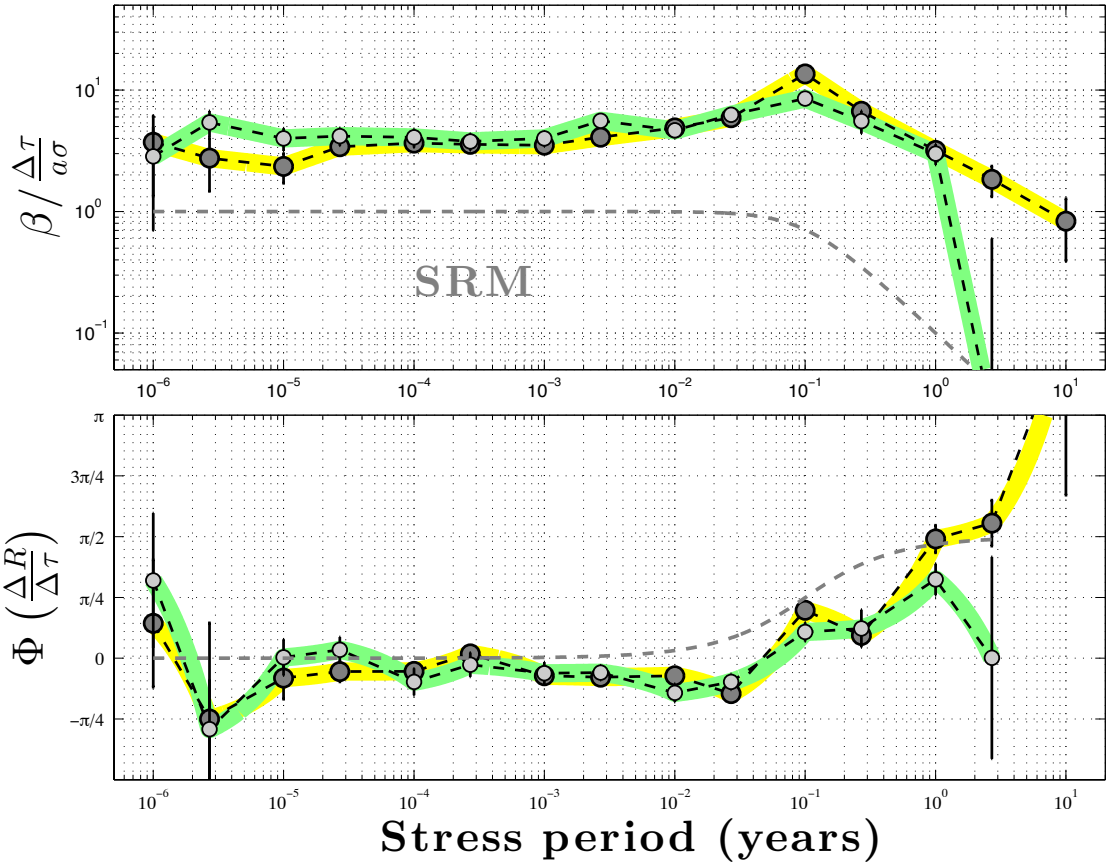

Figure S4: Comparison of the frequency response of faults with creeping zones of different sizes, for large events rupturing the entire seismogenic patch. The large dark grey circles overlying the yellow curve show the frequency response for the fault presented in section 4 which is the exact same plot as in Figure 12, and where the creeping zone is 1200m wide on each side of the seismogenic patch. The smaller light grey circles overlaying the green curve show the response for a fault with the same seismogenic patch, but where the creeping zone is only 450 m wide on each side. Both faults display similar responses, indicating that as long as the creeping zone is wide enough to avoid boundary effects, the actual size of the creeping zone does not have any significant impact on the frequency response of the seismogenic patch. Note that the discrepancy at period $T = 2.7$ years is simply due to a different number of events in the simulations.

Procedure to test the randomness of stress-step application time

In order to test whether the distribution of times Δt between the instant where the stress step is applied and the last seismic event on the seismogenic patch can be described by an exponential PDF $p(\Delta t) = \frac{1}{\Lambda}\exp(-\Delta t/\Lambda)$, we follow the method described in the supplementary material of *Ader and Avouac* (2013). To each Δt we associate a Δt^u, which distribution is uniform if $p(\Delta t)$ is the right PDF for the distribution of the Δt:

$$\Delta t^u = \int_0^{\Delta t} p(t)\, dt. \tag{S1}$$

The Δt^u are by construction distributed over [0;1]. We then divide the [0;1] interval into b bins of equal width and compute the standard deviation σ_Λ of the normalized number of Δt^u falling within each bin. Given the number N_s of Δt^u, we know that σ_Λ should follow the distribution (*Ader and Avouac*, 2013):

$$p_s(\sigma_\Lambda) = \frac{2}{\Gamma\left(\frac{b}{2}\right)}\sqrt{\frac{N_s}{2}}^b \sigma_\Lambda^{b-1} e^{-\frac{N_s\sigma_\Lambda^2}{2}}, \tag{S2}$$

which has an expected value $\sqrt{b/N_s} \pm 1/\sqrt{2N_s}$. The computed value of σ_Λ for different values of Λ as well as the expected theoretical value with error bars are plotted in Figure S5, lower plot.

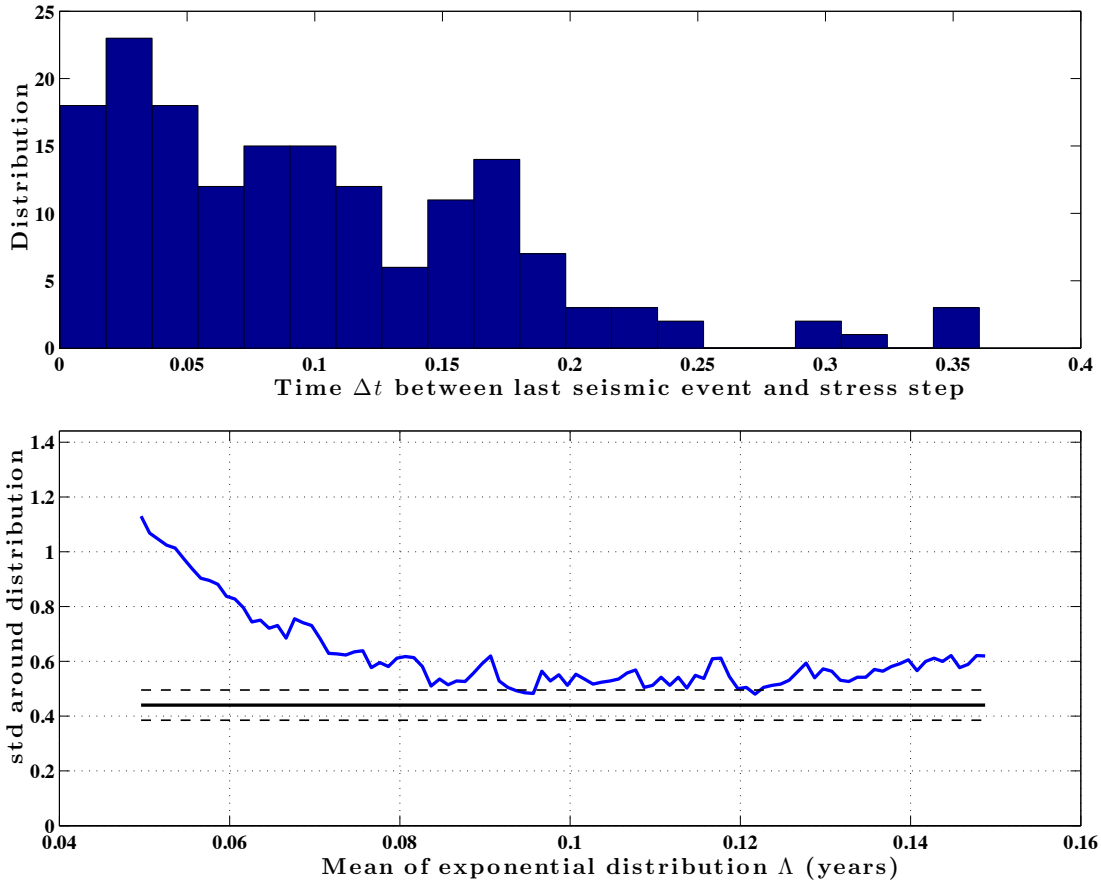

Figure S5: Upper plot: Distribution of times between the last seismic event and the applied stress step. If the stress steps are applied at random times within the seismic cycle, the distribution of these inter times follows an exponential distribution, which mean is half the average inter event time. Lower plot: Test if the distribution of the Δt plotted in the upper plot can occur out of an exponential distribution, of a given mean. The blue line shows the standard deviation of the Δt redistributed along a uniform PDF if their initial distribution results from an exponential distribution of given mean, while the dark blue line indicates the expected the expected standard deviation, with 1-σ deviations indicated by the dashed lines. More details are given in the text.

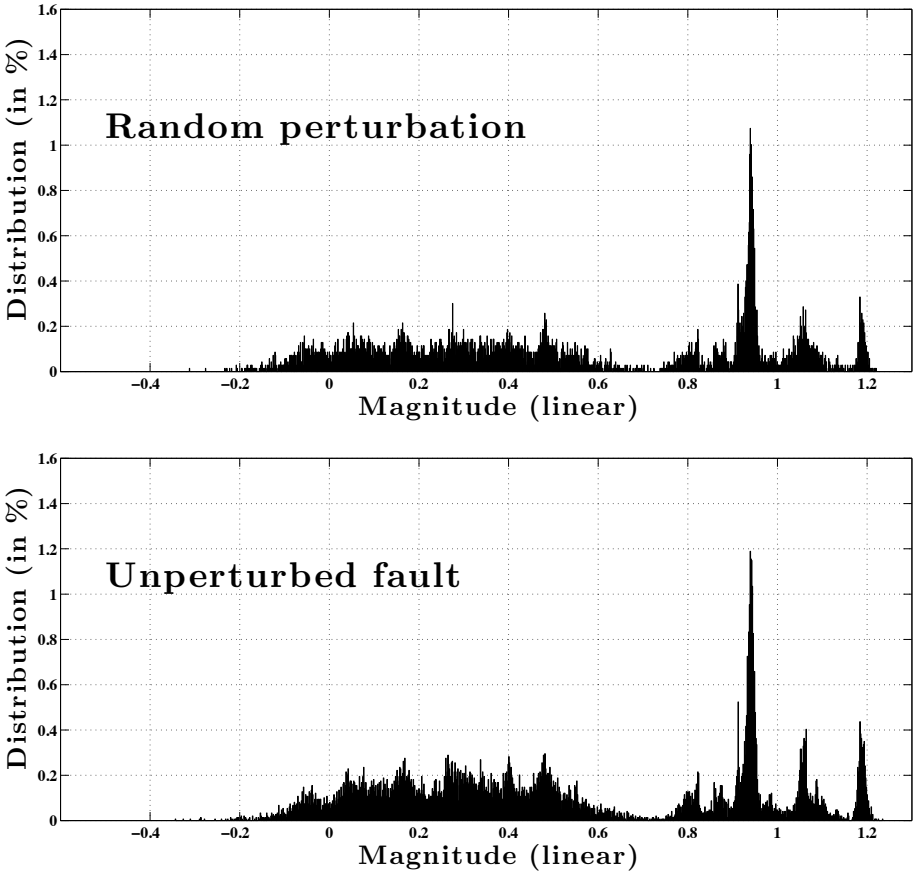

Figure S6: Comparison of the magnitude distribution of the seismic events produced by the seismic patch on a fault undergoing a random perturbation in time. For comparison, the distribution of magnitudes of seismic events produced by the seismic patch on an unperturbed fault (Figure 4b in the main text) is showed on the lower plot, and shows that both distributions are similar. The random perturbation consists of steps of shear stress $\Delta\tau$ of amplitude uniformly distributed between -3 and 3kPa, applied at each time step during the simulation.

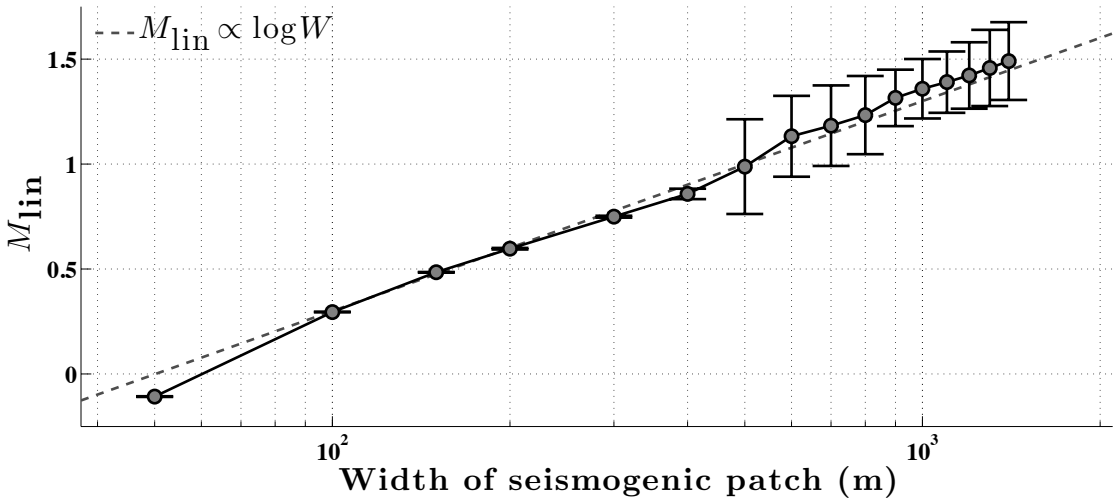

Figure S7: Distribution of linear magnitudes M_{lin} of seismic events that rupture the entire seismogenic patch, as a function of the length of the seismogenic patch. The error bars indicate the spread in magnitudes of events. For patches less than 400 m long, the magnitudes of events are essentially always the same, while some complexity appears for patches longer than 500 m. This plot suggests that, to the first order, M_{lin} is directly proportional to the logarithm of the width of the seismogenic patch. Plugging this relation into equation (11) from the main text leads to $\mathcal{M}_{\mathrm{lin}} \propto W^{3/2}$, which, together with equation (15), indicates that the return period of large events rupturing the entire seismogenic patch depends on its size as $T \propto \sqrt{W}$.

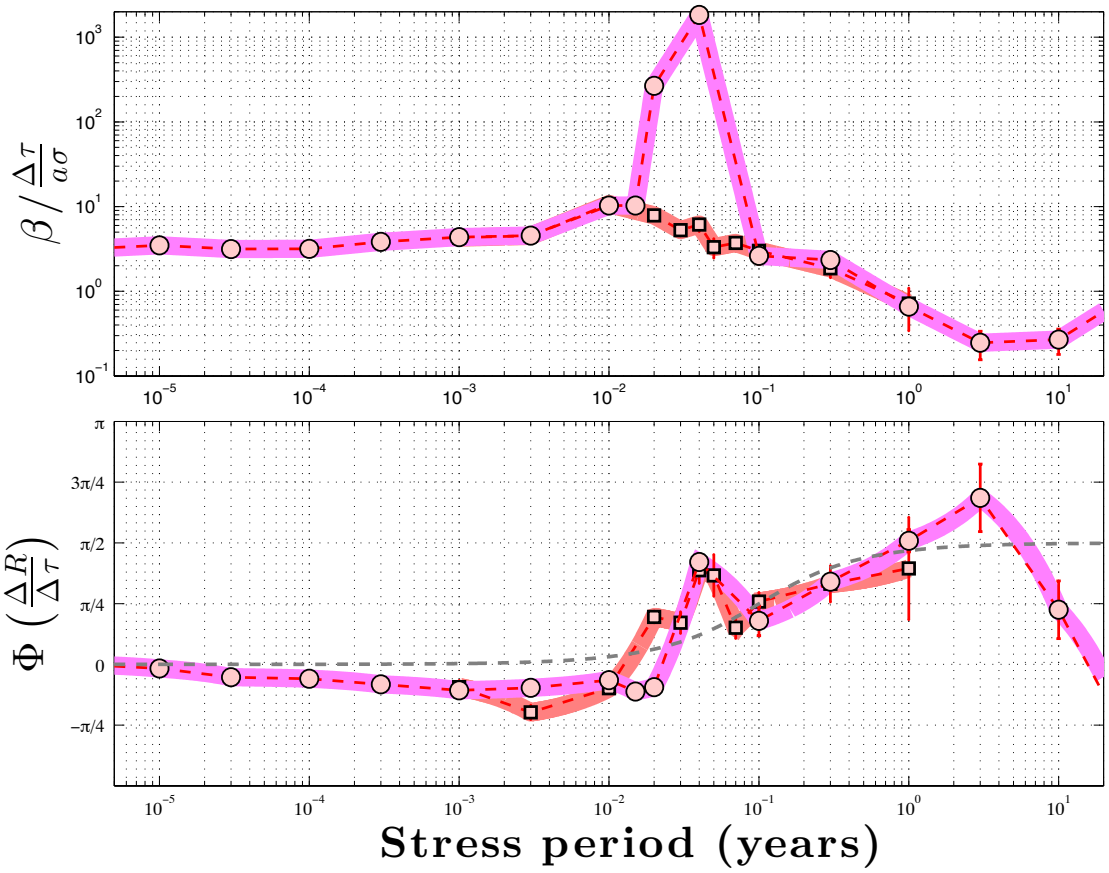

Figure S8: The non-linearity of fault response to harmonic perturbations due to resonances with the return period of characteristic events happening on the fault. In these two simulations, $D_c = 1$ μm and $\sigma = 1$ MPa, similarly to the case of the red squares in Figure 14 from the main text. In this Figure, only the amplitude of the stress perturbation $\Delta\tau$ is changed between the two curves: $\Delta\tau = 0.6$ kPa for the red squares (exactly same plot as red squares in Figure 14) while $\Delta\tau = 3$ kPa for the red circles with purple line. For $\Delta\tau = 0.6$ kPa, the peak response occurs at $T \approx 0.01$ years. For $\Delta\tau = 3$ kPa, this peak is still present, but a much more prominent peak appears at $T \approx 0.05$ years, which is the return period of typical large events produced by the fault. Hence, assessing only the results from $\Delta\tau = 3$ kPa, we would estimate $T_a \approx 0.05$ years, whereas there is another peak for this fault model at 0.01 years. In that sense, the resonance obstructs the determination of T_a. This resonance can also be noted when $\Delta\tau = 0.6$ kPa but is of a much smaller amplitude. When $\Delta\tau = 3$ kPa, this resonance impairs the determination of the critical period T_a, similarly to what happens at $D_c = 10$ μm in Figure 13 from the main text (blue triangles).

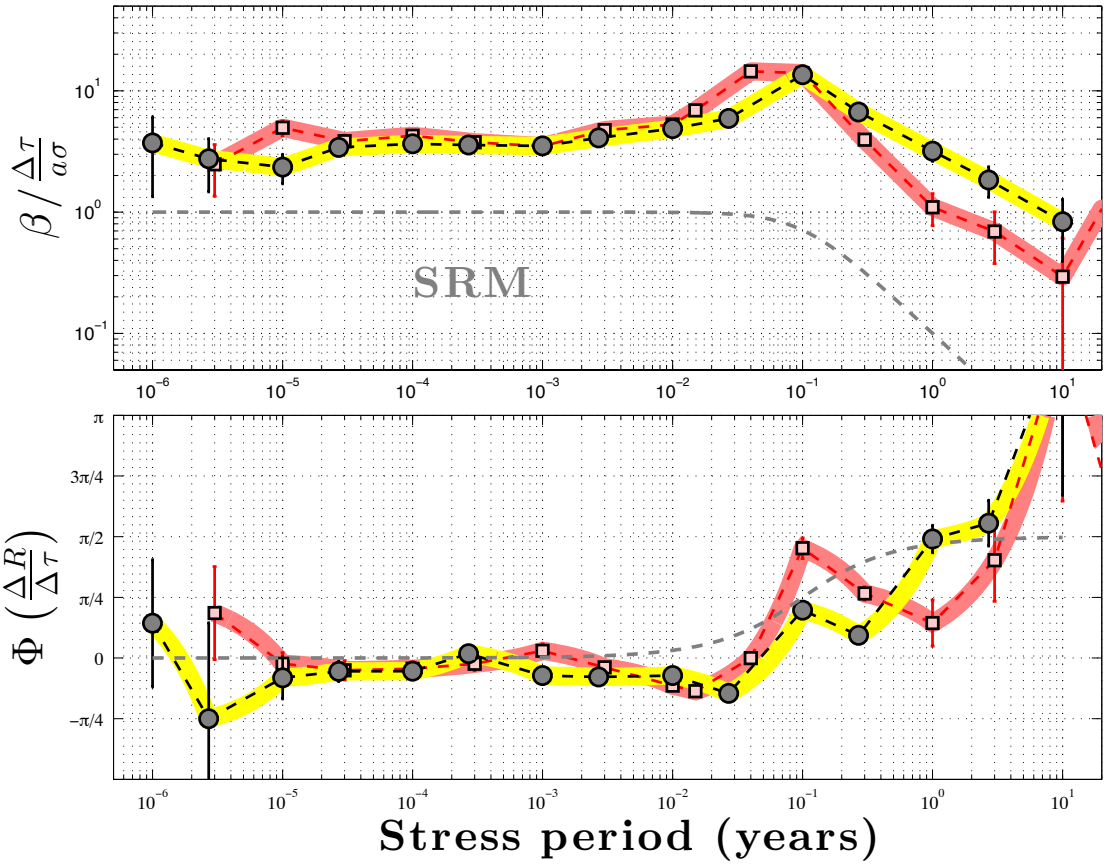

Figure S9: The increase of response of the seismogenic patch around period T_a for different properties of the rate-strengthening zone. The large dark grey circles overlying the yellow curve give the frequency response for the fault presented in section 4, which is the exact same curve as in Figure 12, while the pink squares overlaying the red curve give the response of a similar fault, where the fault properties in the rate-strengthening zone are $b = 0$, such that $a - b = a$. *Ader et al.* (2012) showed that the amplitude of the slip-rate variations in the creeping zone could be inversely proportional to a or $a - b$, depending on the perturbing period, which could result in some cases into an increase of amplitude with the perturbing period. However, the peaked response around T_a is not due to the increase of the variations of slip rate in the creeping zone, since it would be absent in the case of $b = 0$.

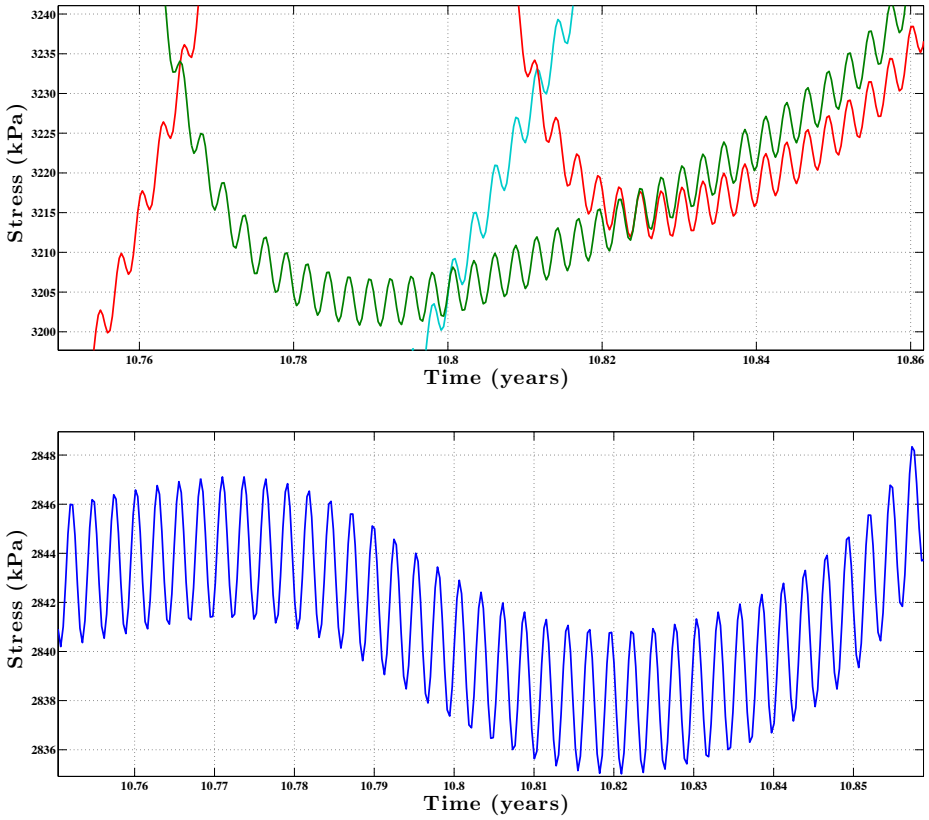

Figure S10: Upper plot: Stress on the fault in the seismogenic patch, with the color corresponding to fault positions from supplementary Figures S2 and S3, for a 3-kPa-stress perturbation at $T = 0.0027$ years. These positions are close to the position of the crack tip at the time of earthquake initiation. Lower plot: Stress on the fault at the rate-weakening/rate-strengthening transition for the same perturbation. On both plots, the amplitude of the stress oscillation on the fault is similar to the amplitude of the imposed oscillatory load, 3 kPa, which shows that there is no significant additional amplification due to the stressing from the creeping region.

Bibliography

Ader, T., and J.-P. Avouac (2013), Detecting periodicities in earthquake catalogs using the Schuster test, application to Himalayan seismicity, *Earth and Planetary Science Letters*, *Submitted*.

Ader, T., J.-P. Ampuero, and J.-P. Avouac (2012), The role of velocity-neutral creep on the modulation of tectonic tremor activity by periodic loading, *Geophysical Research Letters*, *39, L16310*, doi:10.1029/2012GL052,326.